Signatures of field-induced Berezinskii-Kosterlitz-Thouless correlations in the three-dimensional manganite $Bi_{0.5}Sr_{0.5}Mn_{0.9}Cr_{0.1}O_3$

Arjun Ashoka,* K. S. Bhagyashree, and S. V. Bhat†
Department of Physics, Indian Institute of Science, Bangalore-560012, India

(Received 21 September 2018; revised 3 May 2019; accepted 16 June 2020; published 20 July 2020)

Despite experimental evidence for the two-dimensional topological Berezinskii-Kosterlitz-Thouless (BKT) transition in superconducting films and ^{4}He superfluid films, the observation of a BKT transition in condensed matter systems has proven to be difficult. Potential signatures of BKT transitions were reported in two-dimensional magnets, however, the observation of a classical BKT transition in nominally three-dimensional systems has naturally not been investigated as the transition requires an underlying XY model with spins confined to a plane. Here we report that the temperature dependence of the electron paramagnetic resonance (EPR) linewidth observed in $Bi_{0.5}Sr_{0.5}Mn_{1-x}Cr_xO_3$ ($x = 0.1$ and 0.04) as well as in certain other three-dimensional (3D) manganites undergoing antiferromagnetic transitions is described satisfactorily by the BKT model. We explain this unexpected observation of signatures of a two-dimensional topological phase transition in 3D systems in terms of an effective two-dimensional XY easy plane anisotropy induced by the magnetic field applied in the EPR experiment that allows for the mediation of long-range vortex-like correlations between spin clusters formed due to phase segregation. This conclusion is supported by a re-analysis of EPR results reported earlier in La-doped $CaMnO_3$ and a nonmanganite compound $BaNi_2V_2O_8$. We infer that field-induced BKT correlations in a 3D system provide a step towards the observation of a BKT transition in a suitably chosen condensed matter system by the application of an appropriate magnetic field.

DOI: 10.1103/PhysRevB.102.024429

I. INTRODUCTION

Ideal two-dimensional (2D) Heisenberg magnets lack long-range magnetic order [1]. However, the XY model shows a topological phase transition at a finite temperature corresponding to binding and unbinding of magnetic vortices [2,3]. While experimental evidence for such Berezinskii-Kosterlitz-Thouless (BKT) transitions was found in ^{4}He superfluid films and superconducting films [4], in condensed matter systems it has been difficult to observe a BKT transition. In the latter, even weak interlayer coupling that is invariably present leads to long-range order, pre-empting the BKT transition in most cases. Above the long-range magnetic ordering temperature BKT signatures are discernible as a characteristic exponential temperature dependence of the correlation length of the fluctuations. This was observed, for example, in quasi-2D materials such as $BaNi_2V_2O_8$ and more recently in a generalized BKT analysis of certain chromium spinels which are nominally three-dimensional (3D) systems but where geometric antiferromagnetic frustration is understood to have resulted in the reduction of effective dimensionality [5,6]. We report here electron paramagnetic resonance (EPR) studies which indicate that the Cr^{3+}-doped bismuth strontium manganite $Bi_{0.5}Sr_{0.5}Mn_{1-x}Cr_xO_3$ ($x = 0.1, 0.04$) exhibits classical BKT-like correlations even in the absence of two-dimensionality and frustration of structural origin. We explain this unexpected result in terms of frustration originating in the coexistence of antiferromagnetism and ferromagnetism intrinsic to doped manganites, and more importantly, two-dimensionality induced by the applied magnetic field.

$Bi_{0.5}Sr_{0.5}Mn_{1-x}Cr_xO_3$ (BSMCO) belongs to the class of doped perovskite manganites of the type $RAMnO_3$, where R is a trivalent rare earth/Bi^{3+} ion and A is a divalent alkaline earth ion. These manganites exhibit complex phase diagrams with fragile phase boundaries with structural, transport, and magnetic properties extremely sensitive to the amount and nature of doping. Most manganites are intrinsically inhomogeneous due to the very small difference in the free energies of different phases and show strong tendencies towards phase separation consisting of ferromagnetic (FM) metallic and antiferromagnetic (AFM) insulating domains [7]. EPR linewidth ΔH has been an important probe of spin dynamics in manganites [8]. Here we focus on BSMCO—a system showing AFM transitions, where, as T is decreased towards T_N, ΔH continuously increases, diverging around T_N. Such behavior of $\Delta H(T)$ in manganites was observed in the early report of Granado *et al.*, in $Ca_{1-x}La_xMnO_3$ ($x = 0$, 0.02, and 0.05) [9]. They reported that even the very low level of doping has dramatic effects on the EPR linewidth behavior and therefore on the exchange mechanisms. They reported difficulty in fitting their data to the commonly used Ginzberg-Landau critical model [10], according

*Present address: Cavendish Laboratory, University of Cambridge, J. J. Thomson Avenue, Cambridge CB3 0HE, United Kingdom.
†Corresponding author: svbhat@iisc.ac.in

to which,

$$\Delta H(T) = \frac{C}{\left(\frac{T}{T_c} - 1\right)^p} + mT + \Delta H_0, \quad (1)$$

where T_c is the Neel or Curie temperature, C is a proportionality constant, and p is the critical exponent that depends on the underlying spin and spatial degrees of freedom and theoretically takes values between 0.6 and 5.6 for a 3D Ising ferromagnet and a 2D Ising ferromagnet, respectively [11]. A term linear in T and a temperature-independent term are added in Eq. (1) to describe the physics far away from the transition [5]. Granado *et al.* found that Eq. (1) fits the data for the $x = 0.05$ sample satisfactorily, but it cannot fit the data for the $x = 0$ sample.

For the latter sample, they found that the spin freezing model [12] fits better. This formalism leads to an exponential temperature dependence of the linewidth function [12]

$$\Delta H(T) = A \exp\left[-\frac{(T - T_S)}{T_0}\right] + mT + \Delta H_0, \quad (2)$$

where A is a proportionality constant, T_S is the critical transition temperature, e.g., T_N, and T_0 is an empirical constant. We argue that the effectiveness of this model in describing the data of $CaMnO_3$ is fortuitous and the data can be understood with more physical insight via a field-induced BKT scenario as an extension of our BSMCO systems.

In recent work Hemmida *et al.* [6], reported that $\Delta H(T)$ in 3D chromium spinels can be explained by the manifestly 2D BKT scenario. This gives the temperature dependence of the correlation length as [3]

$$\xi = \xi_0 \exp\left[\frac{b}{\left(\frac{T}{T_{\rm BKT}} - 1\right)^{0.5}}\right], \quad (3)$$

where, $T_{\rm BKT}$ is the BKT transition temperature, ξ_0 is the infinite temperature correlation length, and b takes the value of $\pi/2$ for a square lattice [3]. In general, an EPR experiment probes the dynamic structure factor at approximately zero momentum $\mathbf{q}$ (microwave radiation) [6]. Following Benner and Boucher [11], assuming that the average vortex velocity $\bar{u}$ is temperature independent, and with $\gamma = \sqrt{\pi}\bar{u}/2\xi$ we have $\Delta H \propto S_{\mathbf{xx}}(\mathbf{q} \to 0, \omega \to 0) \propto \xi^2/\gamma \propto \xi^3$. Using Eq. (3), we then obtain

$$\Delta H(T) = \Delta H_\infty \exp\left[\frac{3b}{\sqrt{\left(\frac{T}{T_{\rm BKT}} - 1\right)}}\right] + mT + \Delta H_0. \quad (4)$$

Layered magnets with strong in-plane coupling J and a weak interplane coupling J' giving rise to quasi two-dimensionality for the spin degrees of freedom were studied to look for the realization of the BKT transition [5,13]. It was shown that only fluctuations on length scales less than the order of $L_{\rm eff} = \sqrt{(J/J')}$ are two-dimensional in these layered magnets [13] which provides a measure of planar anisotropy that suggests the following expression for systems with weak in-plane anisotropy and interplane coupling:

$$\frac{J}{J'} = \exp\left[\frac{2b}{\sqrt{\frac{T_N}{T_{\rm BKT}} - 1}}\right]. \quad (5)$$

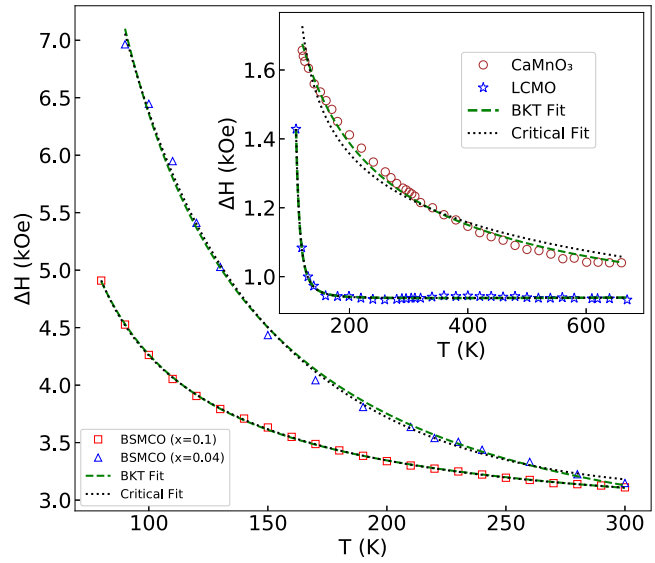

FIG. 1. BKT and critical model fits for BSMCO ($x = 0.1$ and 0.04). Inset: BKT and critical model fits for $CaMnO_3$ and LCMO.

In typical weakly anisotropic layered 2D Heisenberg magnets, J/J' is in the range of 10^3–10^4 [5].

II. EXPERIMENTAL METHODS

The preparation and structural and magnetic characterization of polycrystalline powders of bulk BSMCO ($x = 0.1$) are reported in [14] and BSMCO ($x = 0.04$) is reported in the S1 and S2 of the Supplemental Material [15]. EPR measurements were performed using a commercial X-band spectrometer working at a nominal frequency of 9.4 GHz. ΔH was determined by fitting the data as described in [14] to the broad lorentzian lineshape function which describes the data well until ~70 K in both the samples.

We compare fits of the critical and BKT models to $\Delta H(T)$ for BSMCO in Fig. 1 along with those for $CaMnO_3$ and $La_{0.05}Ca_{0.95}MnO_3$ (LCMO) [9]. Table I, which also includes the results for the exponential model, summarizes the fit parameters and the goodness of fit (R^2 value). Graphical data of $\Delta H(T)$ for $CaMnO_3$, LCMO and $BaNi_2V_2O_8$ were digitized and the errors in the digitized data were calculated to be $\delta(\Delta H) \simeq 2.9$ Oe and $\delta T \simeq 2$ K, both within the errors in the original data implying an ideal or near-ideal reproduction of the published data through digitization.

III. RESULTS

A previous study on the static susceptibility in $x = 0.1$ BSMCO by Bhagyashree *et al.* reported that in this sample short-range FM order coexists with AFM order [14]. This is understood as a FM spin clustering phase in a nominally AFM matrix and manifests as a sharp increase in the field cooled magnetization curve as well as a positive value of 25 K for the Weiss temperature Θ in the Curie-Weiss fit to $\chi = \frac{C}{T-\Theta}$. For the $x = 0.04$ sample we find that the static susceptibility and magnetization results are more ambiguous. The sample is paramagnetic down to $\simeq$50 K where the dM/dT

TABLE I. Summary of fit parameters and goodness of fit for each model. The starred parameters were constrained to within reasonable range of physically realistic or experimentally known values.

Parameter from fit	$CaMnO_3$	LCMO	BSMCO ($x = 0.1$)	BSMCO ($x = 0.04$)
		Critical model		
C (kOe)	1.35	0.0052	3.846	5.221
p	0.14	2.82	0.24	0.68
T_N* (K)	102.0	92.4	56. 9	48.0
m (kOe/K)	0.0	2.1×10^{-6}	1.4×10^{-3}	0.0
ΔH_0 (kOe)	0.00	0.93	2.2×10^{-5}	1.39
R^2	0.98489	0.99925	0.99912	0.99765
		BKT model		
ΔH_∞ (kOe)	0.73	0.0001	0.28	0.79
b*	1.570	1.572	1.572	1.572
T_{BKT} (K)	3.5	83.0	14.7	12.8
m (kOe/K)	0.0	7.5×10^{-6}	0.0	0.0
ΔH_0 (kOe)	0.00	0.93	2.29	0.781
R^2	0.99689	0.99918	0.99986	0.99815
		Exponential (spin freezing model)		
A (kOe)	0.67	6.54	0.24	1.86
T_0 (K)	186.3	8.60	55.5	57.8
T_N* (K)	111.3	87.3	102.1	11.0
m (kOe/K)	0.0	0.0	0.0	0.0
ΔH_0 (kOe)	2×10^{-6}	0.94	3.12	1.25
R^2	0.99959	0.99782	0.99752	0.99933

shows a transition to a magnetically ordered state (Fig. S2 [15]). On first inspection, the ordered state appears to be different from the $x = 0.1$ sample as indicated by the negative Weiss temperature, i.e., $\Theta \simeq -50$ K (Fig. S3 [15]). But it is significantly positively offset with respect to the value for undoped BSMO ($\Theta = -85$ K) indicating the coexistence of the AFM and FM order [16,17]. In this sample the coexistence is less obvious compared to the $x = 0.1$ sample as AFM behavior appears to be dominant with the underlying FM character not strong enough to change the sign of the intercept of the inverse susceptibility.

Magnetization being a static bulk probe is sensitive to global stochiometric changes and the lower Cr doping conceivably reduces the number of FM clusters and hence the overall temperature-dependent inverse susceptibility has less contribution from these clusters and approaches the behavior of undoped BSMO. A deeper understanding, however, requires a dynamic local probe—the EPR linewidth.

As shown in Fig. 1, the divergence of the temperature-dependent EPR linewidth for both the $x = 0.1$ and 0.04 samples appears to be qualitatively very similar barring a scaling factor. As noted by Bhagyashree *et al.* [14] for the $x = 0.1$ sample, this behavior is unexpected as in typical manganites with a FM phase where the linewidth typically decreases as the temperature approaches T_C from above, reaches a minimum at $T_{\mathrm{min}} \approx 1.1\ T_C$ and begins to increase again as the temperature is further decreased. This indicates that the local dynamic correlations probed by EPR linewidth in these two materials have the same essential physics despite the apparently different behavior of magnetization.

From Fig. 1 and the R^2 values in Table I it is clear that the BKT model [Eq. (4)] is superior in describing the temperature dependence of the EPR linewidth in the doped BSMCO when compared to the critical model [Eq. (1)] as the values of the critical exponent from the fit are significantly smaller than any theoretically predicted value. We find that T_{BKT} is effectively insensitive to the Cr doping level with $T_{\mathrm{BKT}} = 14.7K$ for $x = 0.1$ and $T_{\mathrm{BKT}} = 12.8K$ for $x = 0.04$. The computed J/J' values using the T_N from the static susceptibility Curie-Weiss fits are also insensitive to the Cr doping level and are of the order of 1 for $x = 0.1$ and for $x = 0.04$ suggesting a lack of any two dimensionality.

IV. DISCUSSION

It is immediately surprising that a classical BKT transition that requires an XY model with two-dimensional spins confined to a plane describes the data well, especially since the intrinsic magnetic anisotropy given by $J/J' \simeq 1$. We explain this by suggesting that in both samples, the externally applied magnetic field as part of the EPR experiment contributes to the onset of planar anisotropy and the FM spin clusters evidenced by the static susceptibility contribute to the formation of vortices that mediate the transition.

Experimental and quantum Monte Carlo simulation based reports of field-induced BKT transitions in layered 2D Heisenberg AFMs argue the applied field breaks the O(3) symmetry in the Heisenberg model reducing it to an O(2) symmetry which gives rise to genuinely XY behavior over an extended temperature region [18,19]. It does this by

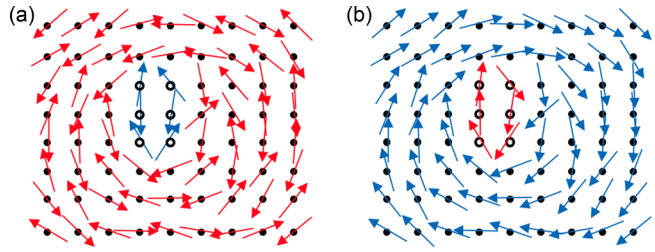

FIG. 2. Schematic showing how a vortex-like structure can be formed as a result of FM-AFM clustering. Here FM nearest-neighbor coupled spins are blue and AFM nearest-neighbor coupled spins are red (color online). These could conceivably lead to the formation of vortex-like spin clusters (at the lattice sites depicted as hollow circles) when projected into two dimensions. (a) Nominally AFM lattice with FM clustering. (b) A staggered magnetization map of (a) for a more conventional vortex representation.

disallowing out-of-plane deformations along the applied field axis, leading to XY behavior and a BKT-like transition. Evidence of a field-induced BKT scenario in a two-dimensional spin dimer system have been reported by Tutsch *et al.* [20]—however, we note that a field-induced BKT transition in 3D systems has not been reported before.

Further, it is also predicted that an arbitrarily small magnetic field can induce a BKT transition and an extended XY phase above it in an isotropic 2D Heisenberg AFM [18,21]. The magnitude of the applied field has a significant impact on the crossover temperature in quasi-two-dimensional compounds and the relation as predicted by renormalization group techniques [22,23] is given by [18] as

$$t_{\mathrm{BKT}} \simeq \frac{4\pi\rho_s/J}{\ln(A/h^2)}, \tag{6}$$

where A is a constant, J is the spin-spin coupling constant, $t = T/J$ is the reduced temperature, ρ_S is the spin stiffness, and $h = g\mu_B H/(JS)$ is the reduced magnetic field where S is $\sqrt{S(S+1)}$.

As shown schematically in Fig. 2, we attribute the formation of vortices required to mediate the transition in the reduced symmetry system to the coexistence of AFM and FM phases in the $x = 0.1$ and 0.04 samples. We suggest that charge ordered Mn^{3+} and Mn^{4+} stripes reported in the undoped parent compound BSMO could conceivably lead to the formation of such spin clusters when doped with Cr^{3+} [24]. This is also evidenced by the positive shift in the intercept of the temperature dependence of the inverse static susceptibility for both samples from the undoped parent compound. We note that the possibility of impurities promoting the formation of spin vortices that could mediate a BKT transition has also been reported in a theoretical study of the $n = 0$ landau Level of graphene by Nomura *et al.* [25]. These Cr^{3+} driven spin cluster vortex-like topological defects required for a BKT transition cannot be removed by moving spins out of the plane without considerable free energy cost from the Zeeman energy due to the external magnetic field, confining them to the plane.

We test the validity of this field induced BKT transition in 3D manganites by extending it to published data on two well-known manganite systems, $La_xCa_{1-x}MnO_3$ for $x = 0$ and $x = 0.05$, reported by Granado *et al.* [9] where they reported that the critical model failed to describe $\Delta H(T)$.

It is clear from Fig. 1 (inset) that applying the critical model, i.e, Eq. (1) is not satisfactory in fitting the experimental data for $CaMnO_3$ consistent with the report by Granando *et al.*, and the coefficient of determination (R^2) of the BKT and exponential models indicate that both outperform the critical model for $CaMnO_3$ (see Table I). We suggest that the good fit of the exponential model, i.e., Eq. (2) with T_N at the magnetization value reported by Granado *et al.* [9] can be misleading as there is no *a priori* way to determine the value of A in Eq. (2). This leaves the exponential term factorizable with two free prefactors as

$$A\exp\left[-\frac{T-T_N}{T_0}\right] = A\exp\left[\frac{T_N}{T_0}\right]\exp\left[-\frac{T}{T_0}\right]. \tag{7}$$

As there is no way to fix the value of A, an empirical parameter, the term $\exp(T_N/T_0)$ serves merely as a scaling factor and does not influence the behavior of the function with respect to T. Only the product $A\exp(T_N/T_0)$ is optimized in any fit, leaving the value of T_N free as long as A is scaled appropriately. Further, this form of a linewidth function does not diverge at $T = T_N$, which is contrary to an EPR observation of the linewidth near an AFM transition, where the signal is expected to disappear [6,26] and hence $\Delta H \to \infty$. We therefore dismiss this form of the linewidth as a useful reflection of the physics of this system which is known to have a clear AFM transition probed by heat capacity and magnetization measurements [27,28]. Using the values obtained from the BKT fit and T_N as 130 K as reported in [28] in Eq. (5), we get a J/J' value of the order of 1, which is consistent with the notion of $CaMnO_3$ as a 3D manganite.

From Fig. 1 (inset) and the R^2 values in Table I for $La_{0.05}Ca_{0.95}MnO_3$ (LCMO), it is clear that the critical model and BKT model are equally satisfactory in describing the data. This is understood by noting that an approximation of the theoretical expression for the BKT transition, i.e., Eq. (4) by critical behavior yields $p \leqslant 3b/2 \simeq 2.4$ [5]. Furthermore, the critical exponent is indicative of the dimensionality of the fluctuations and theoretical calculations predicted that for the 3D Heisenberg AFM $p = 1.7$, for the 3D Ising AFM $p = 1.8$, and for the 2D Ising AFM $p = 3.3$ [11]—all of which differ from our experimental value of 2.8. Our value, $p = 2.8$ is close to the experimentally reported critical exponent $p = 2.6$ in several 2D magnets all of which are considered to be good realizations of weakly anisotropic layered 2D Heisenberg antiferromagnets [5,11]. This is supported by the J/J' value found from Eq. (5) using $T_N = 95$ K as reported in [9], which gives $J/J' \simeq 10^3$, which is of the order typically reported for weakly anisotropic layered 2D Heisenberg antiferromagnets [5]. We conclude that this is strong evidence for the onset of some kind of two-dimensionality in LCMO which appears to behave as a weakly anisotropic layered 2D Heisenberg antiferromagnet.

We take the satisfactory fit of the BKT model to $\Delta H(T)$ of all four 3D manganites, especially in cases where conventional models fail, as preliminary evidence that the externally applied magnetic field as part of the EPR experiment contributes to the onset of planar anisotropy, as this is the only

source of anisotropy that could lead to an effective XY model in all four nominally 3D systems.

To understand if the EPR experiment's applied magnetic field is indeed large enough to induce a BKT transition, we quantify the competition between temperature related fluctuations and the applied magnetic field induced anisotropy energy. We introduce a dimensionless constant η,

$$\eta = \frac{[\mu \cdot H] + i}{k_B T}, \tag{8}$$

where i is some measure of an intrinsic anisotropy energy linked to the sample's magnetic, structural and doping anisotropies, H is the applied magnetic field of the EPR experiment and $k_B T$ represents the thermal fluctuation energy. When $\eta \gg 1$, the two dimensionality of the sample is induced as the thermal fluctuations along the applied magnetic field direction are much smaller than the magnetic interaction and intrinsic anisotropy energy and when $\eta \ll 1$, the sample is isotropic as thermal fluctuations dominate. At $T = T_{\mathrm{BKT}}$ from the fits, $H = 0.335$ T (value of resonance field in X band for LCMO and BSMCO) and setting $i = 0$ we find that $\eta \simeq 0.1$ for $CaMnO_3$ [9]. We justify setting $i = 0$ in $CaMnO_3$ due to the complete lack of any doping and intrinsic anistropy. We interpret $\eta \simeq 0.1$ as an indication that the onset of two-dimensional and consequent BKT-like behavior occurs when the field interaction energy is close to the order of the thermal energy. For the same applied field in BSMCO and LCMO [9], we find T_{BKT} is larger, implying a large value for i in both assuming η to be universally indicative of a BKT onset threshold. We attribute this nonzero intrinsic anisotropy to the presence of dopants that results in inhomogeneous magnetism and phase separation consisting of AFM background and FM clusters [29], driving the formation of vortices. In line with our proposal of spin-cluster-based vortex-like structures in doped BSMCO, evidence is also available for the presence of nanometric scale spin clusters in LCMO [30]. Discussing the difference in the value of i for BSMCO and LCMO is beyond the scope of this study.

To further test our hypothesis that the applied EPR field is responsible for the onset of BKT-like behavior in manganites, we predict that a higher EPR field allows for a higher temperature onset of the threshold anisotropy required for BKT behavior which will manifest as a higher T_{BKT} as predicted by both Eqs. (6) and (8). We consider for an example the results of Heinrich *et al.* of $\Delta H(T)$ [5] probed in X (9.4 GHz) and Q (34 GHz) bands for $BaNi_2V_2O_8$ (BNVO) as the data are available for significantly different applied fields. BNVO is not a manganite but can be used to test the hypothesis which does not require the sample to be a manganite.

For both sample orientations ($H \perp c$ and $H \parallel c$), we have fit the Q and X band probed $\Delta H(T)$ to Eq. (4) with $b = \pi/2$. From Fig. 3 it is immediately apparent that the X band $\Delta H(T)$ diverges at a lower temperature for the $\perp c$ data and we found consistent results for the $\parallel c$ $\Delta H(T)$ data. These fits yield $T_{\mathrm{BKT}_{Q\perp}} = 43.3$ K and $T_{\mathrm{BKT}_{Q\parallel}} = 40.3$ K for the Q band (the same as reported by Heinrich *et al.*) and $T_{\mathrm{BKT}_{X\perp}} = 29.9$ K and $T_{\mathrm{BKT}_{X\parallel}} = 34.8$ K for the X band. Heinrich *et al.* suggested that their X band data may not be reliable as the linewidth value is of the order of the resonance field at low temperature. In

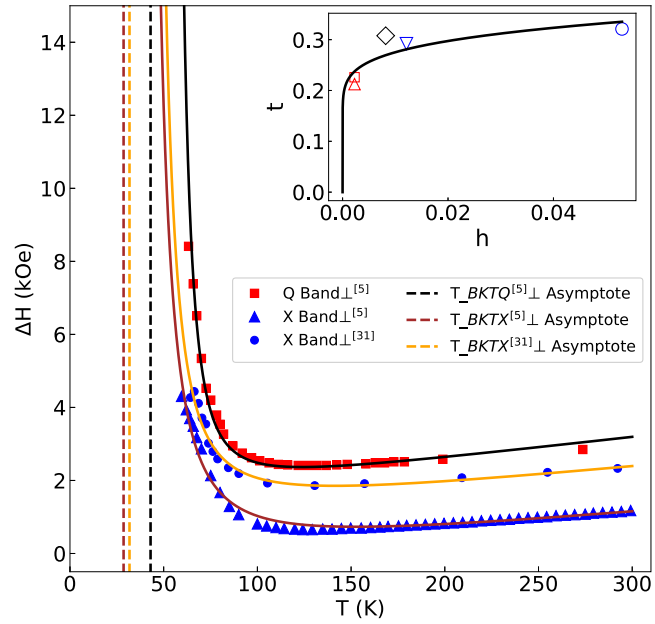

FIG. 3. X-Band ($\perp c$) ΔH fits for $BaNi_2V_2O_8$ reported in [5] and [31] and Q-Band ($\perp c$) ΔH Fits for $BaNi_2V_2O_8$ reported in [5]. Inset: Eq. (6) predicted field dependence fit of Q band (1.08 T) (◊), X band (0.30 T) (△) EPR t_{BKT} from [5], X band (0.30 T □) EPR t_{BKT} from [31], and NMR extracted t_{BKT} at 1.6 T (▽) and 7.0 T (◯) from [31].

view of this we fit X band EPR $\Delta H(T)$ data from a more recent study by Waibel *et al.* on the same compound (also plotted in Fig. 3) [31]. From their X band $\perp c$ data we find $T_{\mathrm{BKT}} = 31.8$ K which is consistent with our analysis of the X band data from Heinrich *et al.* and again significantly lower than the value for Q band in [5].

Using the reported value of $g_\perp = 2.243$ for Ni^{2+} system [5], the magnetic field at the Q and X bands were calculated to be $H_Q = 1.08T$ and $H_X = 0.30T$, respectively, confirming that an increase in the applied field results in an increase in the threshold anisotropy onset temperature and consequently T_{BKT}. The J/J' values calculated (using $T_N = 50$ K as reported in inelastic neutron scattering measurements) [32], for this sample are significantly field dependent, with the Q-Band($\perp c$) $J/J' \simeq 3000$ and the X-Band($\perp$ c) $J/J' \simeq 40$, further confirming the dependence of the planar magnetic anisotropy on the value of the applied magnetic field. We calculate the i from Eq. (8) for both $\perp c$ and $\parallel c$ for $BaNi_2V_2O_8$ to be of the order of an electron's magnetic interaction energy.

We fit Eq. (6) to calculated $t_{\mathrm{BKT}X\perp}$, $t_{\mathrm{BKT}Q\perp}$ and their respective h_X and h_Q as well as NMR longitudinal relaxation time signalled BKT transition temperatures at 1.6 and 7 T extracted from the data reported in [31] using the nearest-neighbor magnetic exchange interaction energy for $BaNi_2V_2O_8$ reported by Klyushina *et al.*($J = 12.125$ meV) [33]. We find the spin stiffness $\rho_S = 0.408J$ from our fit in Fig. 3 (inset), which is the same order of magnitude as the $S = 1/2$ isotropic Heisenberg AFM value of $0.18J$ reported in [34]. We expect that more (h, t) points and including J_{nn} and J_{nnn} interactions will lead to a more precise ρ_S value for this $S = 1$ lattice.

V. CONCLUSION

In summary, we show that when measuring spin fluctuations captured by the dynamic structure factor measured in EPR, the EPR experiment's own applied magnetic field combined with the sample's intrinsic anisotropy can lead to strong signatures of a BKT transition in 3D samples—specifically in the case of BSMCO. We suggest that the applied magnetic field leads to an effective symmetry reduction and genuinely XY behavior by energetically disallowing the removal of vortex-like topological defects at $T \leqslant T_{\mathrm{BKT}}$. We suggest that the physical origin of the vortices arise from magnetic inhomogeneity and spin clusters in these samples. This can be confirmed by inelastic neutron scattering experiments. The relationship between T_{BKT} and the applied field is even seen in $BaNi_2V_2O_8$, a quasi-2D AFM with a calculated high intrinsic planar anisotropy. We conclude that the applied field has significant influence even when intrinsic two-dimensionality is present in the system and thus provides tuneable XY behavior in magnetic insulators [6,19]. This enables us to conclude that BKT correlations can be induced by a magnetic field even in a three-dimensional system, paving the way for the observation of a BKT transition in a suitably chosen condensed matter system by the application of an appropriate magnetic field.

ACKNOWLEDGMENTS

We gratefully acknowledge useful discussions with H. R. Krishnamurthy (Indian Institute of Science, Bangalore). S.V.B. and A.A. thank the Indian Academy of Sciences, National Academy of Sciences, India, and Indian National Science Academy.

APPENDIX: FITTING PARAMETERS

The curves were fit by first fitting the high temperature linear behavior and then extended to the whole temperature range with the physically appropriate constraints. The values extracted from the fit and the coefficient of determination R^2 for each fit are also given in Table I.

[1] N. D. Mermin and H. Wagner, Phys. Rev. Lett. **17**, 1133 (1966).
[2] V. L. Berezinskii, Sov. Phys. JETP **32**, 493 (1971).
[3] J. M. Kosterlitz and D. J. Thouless, J. Phys. C: Solid State Phys. **6**, 1181 (1973).
[4] A. M. Goldman, in *40 Years of Berezinskii-Kosterlitz-Thouless Theory* (World Scientific, Singapore, 2013), pp. 135–160.
[5] M. Heinrich, H.-A. Krug von Nidda, A. Loidl, N. Rogado, and R. J. Cava, Phys. Rev. Lett. **91**, 137601 (2003).
[6] M. Hemmida, H.-A. Krug von Nidda, V. Tsurkan, and A. Loidl, Phys. Rev. B **95**, 224101 (2017).
[7] E. Dagotto, T. Hotta, and A. Moreo, Phys. Rep. **344**, 1 (2001).
[8] D. Huber, D. Laura-Ccahuana, M. Tovar, and M. Causa, J. Magn. Magn. Mater. **310**, e604 (2007).
[9] E. Granado, N. O. Moreno, H. Martinho, A. García, J. A. Sanjurjo, I. Torriani, C. Rettori, J. J. Neumeier, and S. B. Oseroff, Phys. Rev. Lett. **86**, 5385 (2001).
[10] A. Oleaga, A. Salazar, M. Ciomaga Hatnean, and G. Balakrishnan, Phys. Rev. B **92**, 024409 (2015).
[11] H. Benner and J. P. Boucher, *Magnetic Properties of Layered Transition Metal Compounds (Physics and Chemistry of Materials with Low-Dimensional Structures)* (Kluwer Academic, Berlin, 1990), pp. 323–378.
[12] S. Bhagat, M. Spano, and J. Lloyd, Solid State Commun. **38**, 261 (1981).
[13] S. T. Bramwell and P. C. W. Holdsworth, J. Phys.: Condens. Matter **5**, L53 (1993).
[14] K. S. Bhagyashree, L. R. Goveas, and S. V. Bhat, Appl. Magn. Reson. **50**, 1049 (2019).
[15] See Supplemental Material at http://link.aps.org/supplemental/10.1103/PhysRevB.102.024429 for more information on the preparation and structural and static magnetic characterization of BSMCO ($x = 0.04$).
[16] C. Frontera, J. L. García-Muñoz, A. Llobet, M. A. G. Aranda, C. Ritter, M. Respaud, and J. Vanacken, J. Phys.: Condens. Matter **13**, 1071 (2001).
[17] H. Woo, T. A. Tyson, M. Croft, and S.-W. Cheong, J. Phys.: Condens. Matter **16**, 2689 (2004).
[18] A. Cuccoli, T. Roscilde, R. Vaia, and P. Verrucchi, Phys. Rev. B **68**, 060402(R) (2003).
[19] L. Baranová, A. Orendáčová, E. Čižmár, R. Tarasenko, V. Tkáč, M. Orendáč, and A. Feher, J. Magn. Magn. Mater. **404**, 53 (2016).
[20] U. Tutsch, B. Wolf, S. Wessel, L. Postulka, Y. Tsui, H. Jeschke, I. Opahle, T. Saha-Dasgupta, R. Valentí, A. Brühl, K. Remović-Langer, T. Kretz, H.-W. Lerner, M. Wagner, and M. Lang, Nat. Commun. **5**, 5169 (2014).
[21] A. Cuccoli, T. Roscilde, V. Tognetti, R. Vaia, and P. Verrucchi, Phys. Rev. B **67**, 104414 (2003).
[22] S. B. Khokhlachev, Sov. Phys. JETP **43**, 137 (1976).
[23] V. Y. Irkhin and A. A. Katanin, Phys. Rev. B **60**, 2990 (1999).
[24] M. Hervieu, A. Maignan, C. Martin, N. Nguyen, and B. Raveau, Chem. Mater. **13**, 1356 (2001).
[25] K. Nomura, S. Ryu, and D.-H. Lee, Phys. Rev. Lett. **103**, 216801 (2009).
[26] H. Martinho, N. O. Moreno, J. A. Sanjurjo, C. Rettori, A. J. García-Adeva, D. L. Huber, S. B. Oseroff, W. Ratcliff, S.-W. Cheong, P. G. Pagliuso, J. L. Sarrao, and G. B. Martins, Phys. Rev. B **64**, 024408 (2001).
[27] J. J. Neumeier, A. L. Cornelius, and K. Andres, Phys. Rev. B **64**, 172406 (2001).
[28] A. L. Cornelius, B. E. Light, and J. J. Neumeier, Phys. Rev. B **68**, 014403 (2003).
[29] C. D. Ling, E. Granado, J. J. Neumeier, J. W. Lynn, and D. N. Argyriou, Phys. Rev. B **68**, 134439 (2003).
[30] E. Granado, C. D. Ling, J. J. Neumeier, J. W. Lynn, and D. N. Argyriou, Phys. Rev. B **68**, 134440 (2003).
[31] D. Waibel, G. Fischer, T. Wolf, H. V. Löhneysen, and B. Pilawa, Phys. Rev. B **91**, 214412 (2015).
[32] N. Rogado, Q. Huang, J. W. Lynn, A. P. Ramirez, D. Huse, and R. J. Cava, Phys. Rev. B **65**, 144443 (2002).
[33] E. S. Klyushina, B. Lake, A. T. M. N. Islam, J. T. Park, A. Schneidewind, T. Guidi, E. A. Goremychkin, B. Klemke, and M. Månsson, Phys. Rev. B **96**, 214428 (2017).
[34] R. R. P. Singh and D. A. Huse, Phys. Rev. B **40**, 7247 (1989).